5.4 SCANNER IMAGING SYSTEMS, AIRCRAFT

Stephen G. Ungar
NASA/Goddard Institute for Space Studies

With the advent of advanced satellite-borne scanner systems, the geometric and radiometric correction of aircraft scanner data has become increasingly important. These corrections are needed to reliably simulate observations obtained by such systems for purposes of evaluation. This paper reviews the causes and effects of distortion in aircraft scanner data and discusses an approach to reduce distortions by modelling the effect of aircraft motion on the scanner scene.

Causes of Distortion

Both the location of an observation (or pixel) on the ground and the target area (footprint) contained within the instantaneous field of view (IFOV) of the sensor system are governed by the following three factors: aircraft position; aircraft attitude; and sensor system can angle. Terrain relief may interact with aircraft/scanner geometry to further complicate determination of pixel position and footprint in planar coordinates. For purposes of this discussion, we shall address only cases in which the terrain effects are negligible.

During the acquisition of a single scan line, the scan pattern on the ground is largely a function of the scan geometry convoluted with the attitude of the aircraft. It is convenient to

characterize an aircraft's attitude (orientation) in terms of a fusilage axis and a wing axis. The fusilage axis passes from tail to nose through the aircraft's center of gravity. The wing axis passes through the center of gravity parallel to the wing surface. The orientation of the fusilage axis is expressed in spherical polar coordinates as follows: the angle of rotation east of north about a vertical axis (clockwise rotation looking down at aircraft) is called heading (ϕ); the angle of the nose above the horizontal is called the pitch (θ). An additional angle, roll (ρ), is required to specify the final orientation of the wing axis and is measured by the degree of clockwise rotation of the aircraft about the fusilage axis looking towards the nose. Since the aircraft scanner systems treated here rotate in a plane perpendicular to the fusilage axis, roll can be combined with the scanner orientation to determine the effective scan angle. The scan angle (ψ) is the look angle of the sensor measured clockwise from a direction mutually perpendicular to the fusilage and wing axis (i.e., the nadir direction for an aircraft in level flight). Therefore, the effective scan angle may be expressed as ($\psi_e = \rho + \psi$).

Given the altitude of the aircraft and the coordinates of the nadir point below the aircraft, the position of the instantaneous viewpoint on the ground can now be located in terms of the attitude parameters. Table 1 presents the detailed formulas required for making this calculation. "h" is the altitude of the aircraft above the ground, X_o and Y_o are the coordinates at aircraft nadir.

We have selected a coordinate system in which the positive x-direction is east and the positive y-direction is south in order to conform to conventions found in most image processing systems.

Impact of Aircraft Motion

In principle, both the attitude and position of the aircraft changes during the acquisition of a scan line. However, contemporary scanner systems actively gather image data only during a time interval of approximately 12 to 28 percent of the scan period. Typical scan periods range from 0.05 to 0.1 seconds. Therefore, in practice, changes in aircraft attitude may be considered negligible during the active portion of the scan. The forward motion of the aircraft will introduce skew in the scan line pattern which amounts to approximately one-tenth pixel displacement at the end of the scan line for contemporary systems. This corresponds to an angle of about 0.01 degrees. A viable geometric correction scheme need only update the aircraft's position once per scan line, specifying the aircraft coordinates at $\psi = 0$.

Rectification of Scanner Data

Table 1 outlines a method for rectifying aircraft scanner observations in cases where reliable navigational data is available. As previously discussed, the first half of the table relates the planar coordinates of the pixel to the navigational parameters for a given nadir location (X_o, Y_o). The remainder of Table 1 describes an integration scheme for updating the nadir position during the course of the flight. The scheme is valid for situations in which navigational data is available at time intervals wnich are com-

parable or less than the scan period. The values of all navigational parameters including aircraft velocity may be estimated at the center of each scan ($\psi = 0$) by cubic interpolation as indicated in Step 2. Finally, the aircraft nadir displacement in both the x and y-directions between scans may be calculated as indicated in Step 3. For roll-compensated systems, the scan mirror moves with a constant "inertial" velocity and Δt represents the period of ($\psi_e = \rho + \psi$). Under these circumstances, the solutions to the equations in Table 1 are equivalent to assuming $\rho = 0$ at all times and dropping that term out of the analysis.

Simulated Flight

The impact of variations in flight parameters on aircraft scanner imagery can best be illustrated by simulating a flight over a geometrically regular pattern and varying the flight parameters in a controlled way. The simulated scanner system selected for this study is patterned after NASA's NS001 scanner system flown onboard a C130 aircraft. Nominal flight and scanner parameters are given in Table 2. Simulated flights are conducted over a checkerboard pattern consisting of half mile square sections (approximately 800 meters x 800 meters). Figures 1(A-L) show the results of such flights with flight parameters deviating from the nominal values as specified. The left portion of each figure displays the scan system pattern projected on the ground as follows: the "footprint" for each observation along every 90th scan line is represented as a plotting point; in addition, the footprints of observations on every scan line are plotted at

10 degree intervals (from -50 to +50 degrees). The scanner "image", consisting of radiometric values of the simulated checkerboard terrain, is displayed in scanner coordinates (pixel position, scan line) to the right of its corresponding ground pattern.

For agricultural applications, it is instructive to draw an analogy between the checkerboard squares and field boundaries. Figure 1(A) represents an ideal case of the aircraft flying from north to south, parallel to field boundaries, with all parameters fixed at constant altitude. The foreshortening of fields at the edges of the flightline is due to the oblique look angle at the ends of the scan. In Figure 1(B), we introduce a drift (v_x component) in the aircraft motion while keeping the heading (orientation) of the aircraft north-south (in positive y-direction). Motion of this sort occurs in situations where aircraft flying at fixed headings are subject to substantial constant cross winds. The drift component introduces a skew in north-south field boundaries caused by the shift in x value of the nadir coordinates along the aircraft ground track. Figure 1(C) illustrates a flight with heading 20 degrees west of south as opposed to due south. This produces a flight pattern identical to that of Figure 1(A), but rotated with respect to field boundaries. The accompanying image shows the typical S-shaped distortion in the field boundaries that is so characteristic of linear features in aircraft scanner data. This occurs because the road sections are no longer aligned with the scan direction, although the

distortion is still in the scan direction. Figure 1(D) portrays the impact of the aircraft flying in a banked position. The scan center ground track is displaced 20 degrees to the west of the aircraft nadir ground track. Many aircraft scanner systems, including the NS001, are "roll-compensated" to maintain the scan center along the aircraft nadir ground track.

Many of the distortions in scanner imagery result largely from *variations* in orientation of the aircraft during the flight. For example, a change in pitch results largely in a fixed displacement along the ground track such that the aircraft is looking somewhat ahead of where it normally would. In addition, each scan covers a somewhat wider swath on the ground. However, variations in pitch results in distortions such as those displayed in Figures 1(E) and 1(H). In Figure 1(E), the pitch varies linearly from 0 degrees at the start of the flight segment to 20 degrees at the end. The most apparent effect is the widening coverage in the scan direction as the flight progresses. In addition, the changing pitch angle contributes to increasing the effective ground velocity beyond v_y. Thus the distance between scan lines is increased, resulting in a squeezing of fields in the y-direction on the scanner image. Figures 1(F) and 1(G) display the impact of similar type variations in heading and drift, and in roll. In particular, Figure 1(F) shows the combined effect of a 10 degree linear variation in heading and a 10 degree linear variation in aircraft tracking angle due to drift.

In general, aircraft motions are more complex than can be adequately represented by a linear variation over the course of the flight. Typically, motion will be oscillatory in nature, since it is generally desirable to correct departures from nominal flight parameters. Figures 1(H) through 1(L) portray the effects of sinusoidal variations in selected flight parameters. In Figure 1(H) the aircraft nose pitches up to a maximum angle of 20 degrees and then is brought back down, passing through the horizontal, to a negative pitch angle of 20 degrees and finally back to horizontal flight by the end of the flight segment. The scan pattern near the center of the flight segment indicates that, although the aircraft is moving forward the center line of the scanner moves backward because of the variation in pitch resulting in a prolonged viewing period for areas on the ground at this point in the flight. This is clearly seen by field distortions in the accompanying image. Figure 1(I shows the result of similar variation in heading. The turning of the aircraft can cause the edges of the scan line to move backward with respect to forward motion of the aircraft during portions of the flight segment. This can result in a rather distorted image since the same area on the ground may be viewed more than once during the flight segment. In effect, at the time the aircraft is experiencing its maximum change in heading, it may be considered as moving perpendicular to a radius of curvature lying along the scan direction. Ground areas near the center of curvature will be observed repeatedly while the edge of the scan, beyond the radius of the curvature, will be covered in reverse

direction (from south to north) during that portion of the flight segment. As the variation in heading is reduced the normal forward motion of the aircraft will force the scan coverage at the edge to once again proceed from north to south doubling back over the area covered. In fact, some areas near the edge of the scan line may be observed as many as three times during the course of the flight segment. This creates a rather significant problem in attempting to recapture or correct for radiometric values, even in the situations where the scanner geometry is well-known.

As can be seen in Figure 1(J), variations in the aircraft tracking angle equal to those occurring in Figure 1(I) can be obtained by varying the drift angle. The scan center ground track in Figure 1(I) is identical to that of 1(J). However, in 1(J) the orientation of the aircraft is maintained constant and the scan pattern is consequently much simpler, with no crossing of scan lines. Figure 1(K) displays a situation in which the heading and drift are varying simultaneously in a manner such that the tracking angle variation is identical to that of Figures 1(I) anf 1(J). Once again, it is difficult to establish a one-to-one mapping between actual ground coordinate radiometric values and the values which appear in the scanner image. Figure 1(L) portrays a sinusoidal variation in roll angle, beginning from level flight, banking to 20 degrees below the horizon in the west, and returing to level flight. In this instance, the flight segment is flown in the time equal to the half period of the sinusoidal variation.

In summary, if sufficient navigational information is available, aircraft scanner coordinates may be related very precisely to planimetric ground coordinates using the approach outlined in Table 1. However, the potential for a multi-value remapping transformation (i.e., scan lines crossing each other), adds an inherent uncertainty, to any radiometric resampling scheme, which is dependent on the precise geometry of the scan and ground pattern.

TABLE 1

AIRCRAFT SCANNER GROUND PATTERN EQUATIONS

$$X = X_o + h \tan\theta \sin\phi - h(\tan(\rho+\psi)/\cos\theta)\cos\phi$$

$$Y = Y_o - h \tan\theta \cos\phi - h(\tan(\rho+\psi)/\cos\theta)\sin\phi$$

$$X_o(t+\Delta t) = X_o(t) + \int_t^{t+\Delta t} v \sin(\phi+\delta)\,dt$$

$$Y_o(t+\Delta t) = Y_o(t) - \int_t^{t+\Delta t} v \cos(\phi+\delta)\,dt$$

where: X_o, Y_o = nadir coordinates

Δt = scan period	ρ = roll
θ = pitch	ψ = scan angle
ϕ = heading	h = altitude
δ = drift	v = ground speed

UPDATING X_o, Y_o WITH NAVIGATION DATA (NERDAS)

(1) Find nearest observation times from NERDAS

$t_i \le t \le t_{i+1}$ where: $i = \text{INT}\{(t-t_o)/f+1\}$

f = frequency of observation

(2) Obtain values for each scan by cubic interpolation

$$Z(t) = \sum_{n=0}^{3} a_n t^n$$

where: Z represents $[\theta, \phi, \delta, \rho, h, \text{or } v]$

using NERDAS values for $Z(t_i)$ $i-1 \le k \le i+2$

solve for a_n $n = 0, \ldots 4$

(3) Calculate nadir displacement between scans assuming

$$\int_t^{t+\Delta t} Z\,dt = \sum_{n=1}^{4} \frac{a_{n-1}}{n}\left\{(t+1/f)^n - t^n\right\}$$

where: Z represents $v \sin(\phi+\delta)$ or $-v \cos(\phi+\delta)$

and a_n is determined by technique used in step (2)

TABLE 2

SIMULATED NS001 FLIGHT
NOMINAL FLIGHT PARAMETERS

DRIFT	$\delta_0 = 0°$
HEADING	$\phi_0 = 180°$
PITCH	$\theta_0 = 0°$
ROLL	$\rho_0 = 0°$
GROUND SPEED	$V_G = 280$ KNOTS
ALTITUDE	$H = 25{,}400$ FEET
SCAN ANGLE	$-50° < \Psi < 50°$
SCAN FREQ.	$F = 15$ RPS
IFOV	$\Omega = 2.5$ MR

FIGURE 1 (A - C)

SIMULATED FLIGHT-SCANNER GROUND PATTERN AND IMAGE

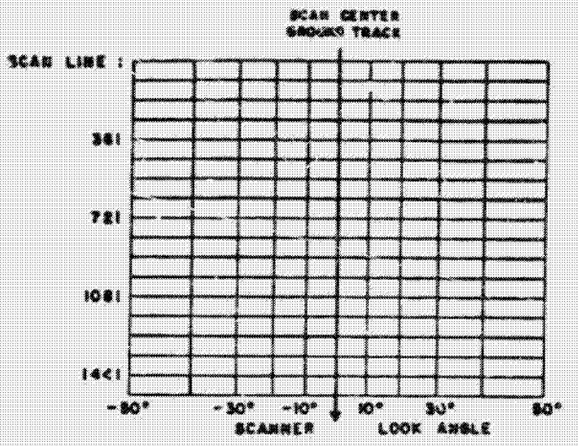

(A)

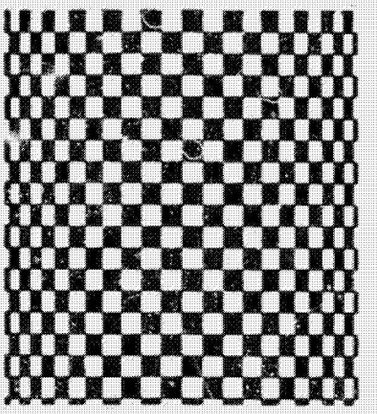

Nominal flight parameters

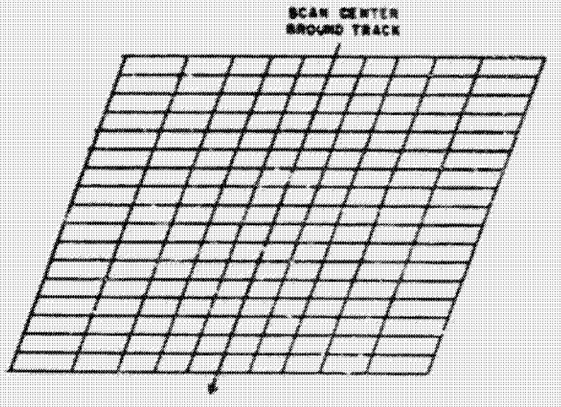

(B)

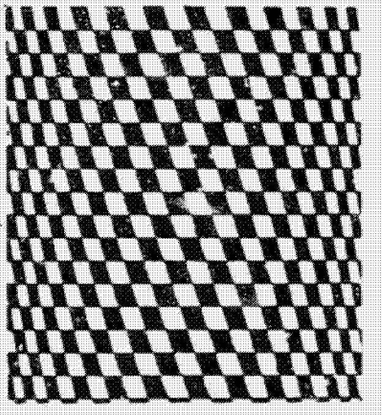

20° change from nominal drift ($\delta = \delta_0 + 20$)

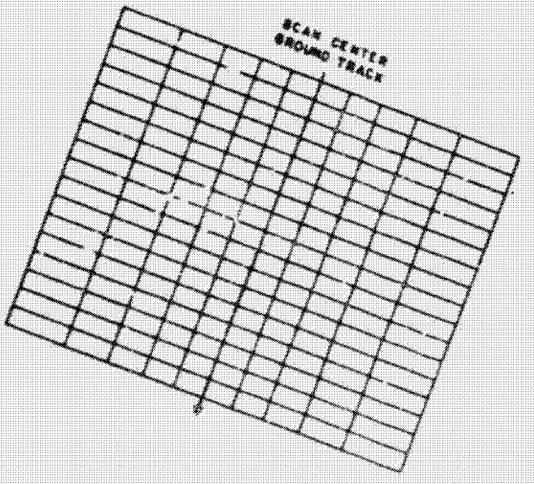

(C)

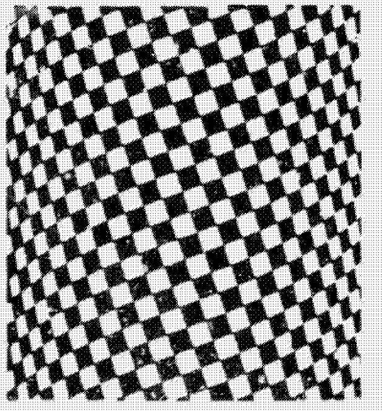

20° change from nominal heading ($\phi = \phi_0 + 20$)

FIGURE 1 (D - F)

SIMULATED FLIGHT-SCANNER GROUND PATTERN AND IMAGE

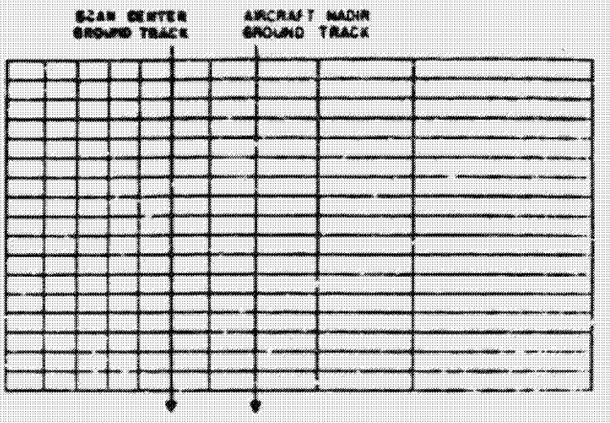

(D)

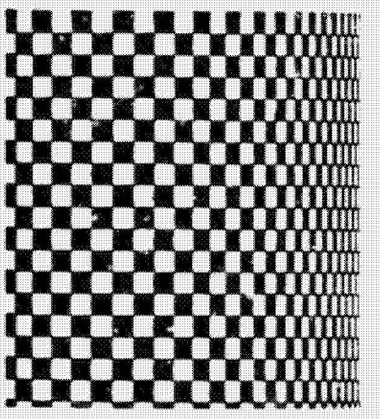

20° change from nominal roll ($\rho = \rho_0 + 20$)

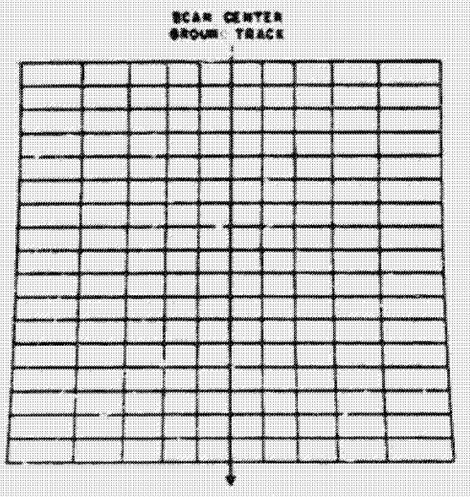

(E)

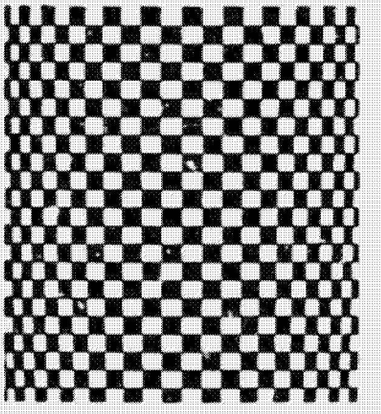

20° linear variation in pitch ($\theta = \theta_0 + 20\alpha t$)

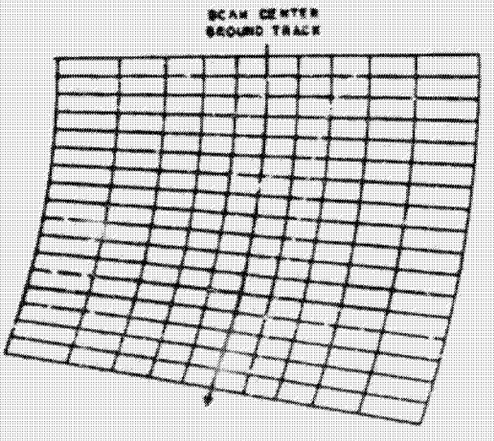

(F)

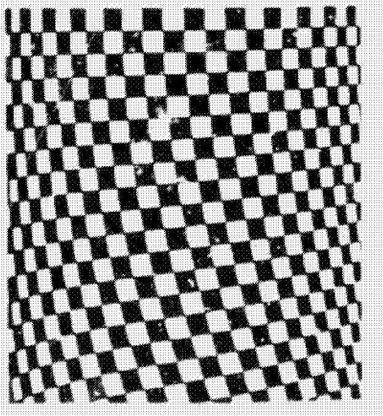

10° linear variations in heading and drift

FIGURE 1 (G - I)

SIMULATED FLIGHT-SCANNER GROUND PATTERN AND IMAGE

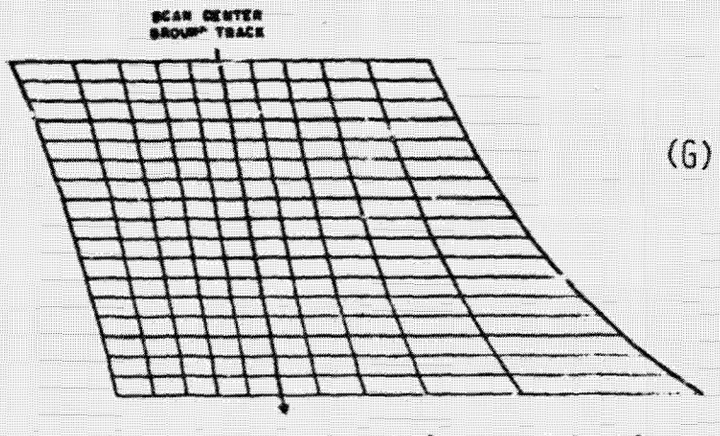

(G)

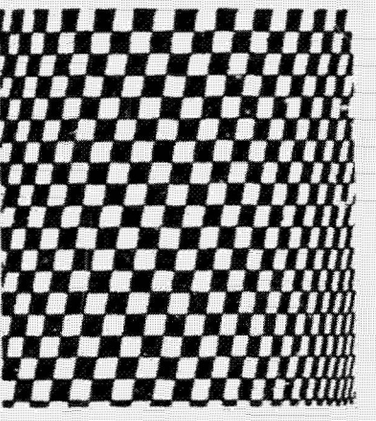

20° linear variation in roll ($\rho = \rho_0 + 20\alpha t$)

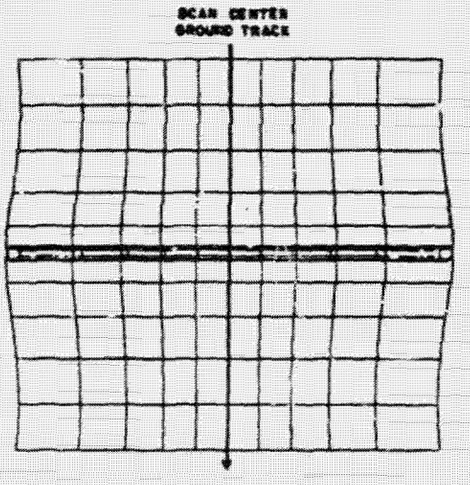

(H)

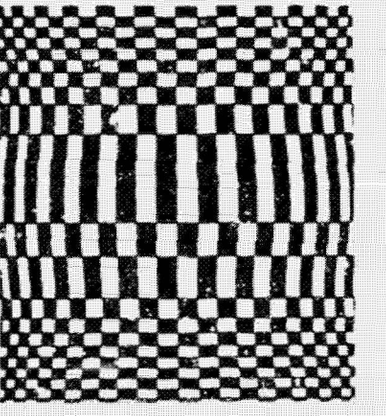

20° sinusoidal variation in pitch ($\theta = \theta_0 + 20 \sin \omega t$)

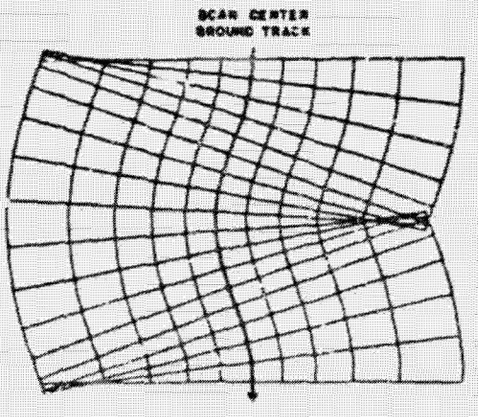

(I)

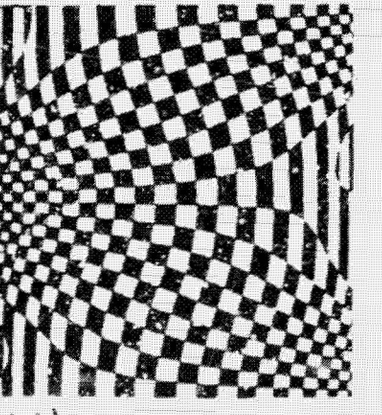

20° sinusoidal variation in heading ($\phi = \phi_0 + 20 \sin \omega t$)

FIGURE 1 (J - L)

SIMULATED FLIGHT-SCANNER GROUND PATTERN AND IMAGE

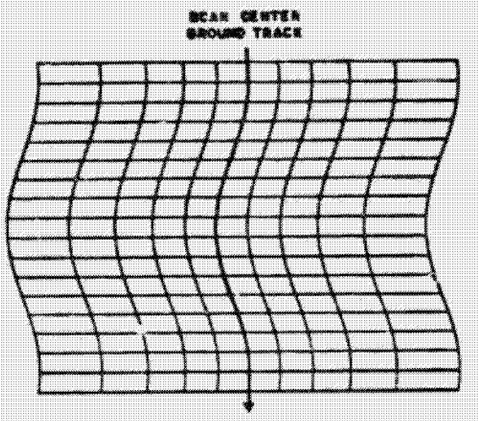

(J)

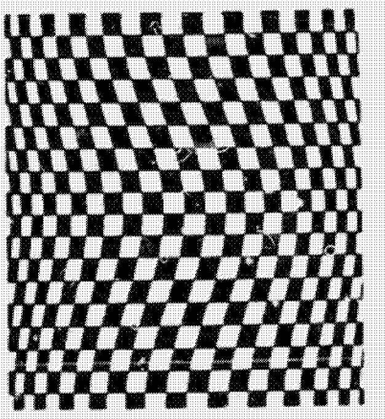

20° sinusoidal variation in drift ($\delta = \delta_0 + 20 \sin \omega t$)

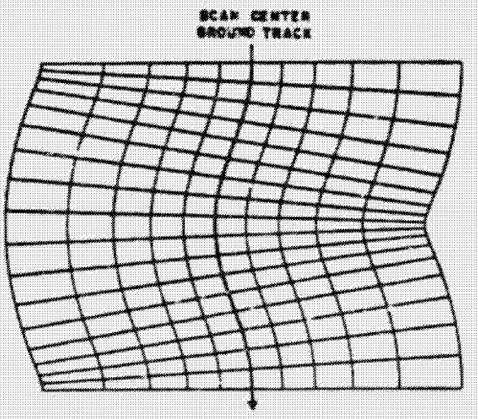

(K)

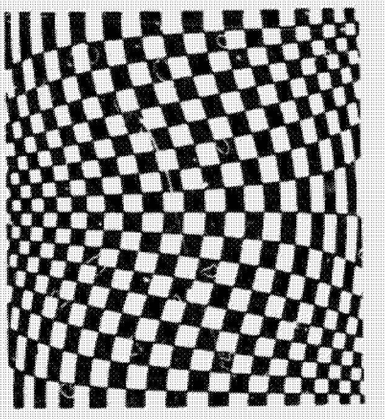

10° sinusoidal variations in heading and drift

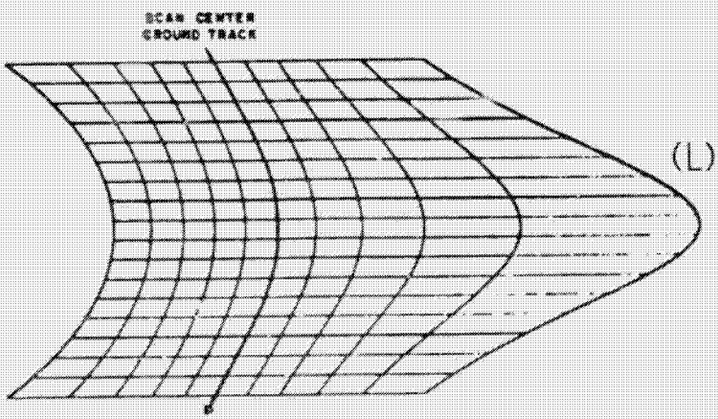

(L)

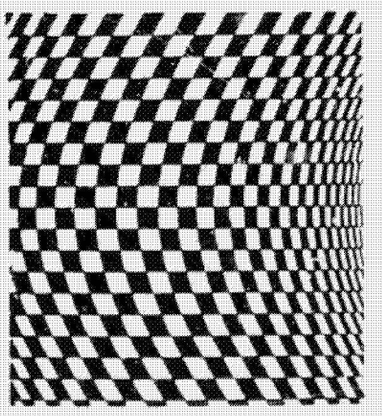

20° sinusoidal variation in roll ($\rho = \rho_0 + 20 \sin \omega t$)